

1 **Global ecomorphological restructuring of dominant marine reptiles prior to the**  
2 **K/Pg mass extinction**

3 **Jamie A. MacLaren<sup>1,2\*</sup>, Rebecca F. Bennion<sup>1,3</sup>, Nathalie Bardet<sup>4</sup>, Valentin Fischer<sup>1</sup>**

4

5 <sup>1</sup> Evolution & Diversity Dynamics Lab, UR Geology, Université de Liège, 14 Allée du 6 Août, 4000 Liège,  
6 Belgium.

7 <sup>2</sup> Functional Morphology Lab, Department of Biology, Universiteit Antwerpen, Gebouw D, Campus Drie  
8 Eiken, Universiteitsplein 1, Wilrijk, 2610 Antwerpen, Belgium

9 <sup>3</sup> O.D Terre et Histoire de la Vie, Institut Royal des Sciences Naturelles de Belgique, Rue Vautier 29, 1000  
10 Brussels, Belgium.

11 <sup>4</sup> CR2P, Muséum National d'Histoire Naturelle, 8 Rue Buffon, CP38, 75005 Paris, France

12 \*corresponding author

13

14

15 Corresponding Author

16 Email Address: [j.maclaren@uliege.be](mailto:j.maclaren@uliege.be)

17 Institutional Address: Building B18, Allée du Six Août 14, Sart-Tilman Campus, Université de Liège, Liège  
18 4000, Belgium.

19

20

21

22

23 **ABSTRACT**

24 Mosasaurid squamates were the dominant amniote predators in marine ecosystems during most of the Late  
25 Cretaceous. Evidence from multiple sites worldwide of a global mosasaurid community restructuring across  
26 the Campanian–Maastrichtian transition may have wide-ranging implications for the evolution of diversity of  
27 these top oceanic predators. In this study, we use a suite of biomechanical traits and functionally descriptive  
28 ratios to investigate how the morphofunctional disparity of mosasaurids evolved through time and space prior  
29 to the Cretaceous–Palaeogene (K/Pg) mass extinction. Our results suggest that the worldwide taxonomic  
30 turnover in mosasaurid community composition from Campanian to Maastrichtian is reflected by a notable  
31 increase in morphofunctional disparity on a global scale, but especially driven the North American record.  
32 Ecomorphospace occupation becomes more polarised during the late Maastrichtian, as the morphofunctional  
33 disparity of mosasaurids plateaus in the Southern Hemisphere and decreases in the Northern Hemisphere. We  
34 show that these changes are not associated with strong modifications in mosasaurid size, but rather with the  
35 functional capacities of their skulls, and that mosasaurid morphofunctional disparity was in decline in several  
36 provincial communities before the K-Pg mass extinction. Our study highlights region-specific patterns of  
37 disparity evolution, and the importance of assessing vertebrate extinctions both globally and regionally.  
38 Ecomorphological differentiation in mosasaurid communities, coupled with declines in other formerly  
39 abundant marine reptile groups, indicates widespread restructuring of higher trophic levels in marine food  
40 webs was well underway when the K-Pg mass extinction took place.

41

42 **Keywords:** Mosasauridae – morphometrics – provincialism – megapredator – ecomorphology – Cretaceous

43

## 44 INTRODUCTION

45 Marine ecosystems were dominated by reptiles during the entire Mesozoic (Motani 2002; Massare 1987;  
46 Bardet 2012; Scheyer et al. 2014). Despite important turnovers at its base (Fischer et al. 2017; 2020), the Late  
47 Cretaceous is no exception, as mosasaurid squamates rapidly diversified (Bardet et al. 2008; 2007; Polcyn et  
48 al. 2014), achieving a cosmopolitan distribution prior to the Campanian (c.83.5 Mya) (Bardet et al. 2014;  
49 Polcyn et al. 2014), and colonised several ecological guilds until their global extinction at the K/Pg boundary  
50 mass extinction (66 Mya) (Martin et al. 2017). Prior to the Campanian, mosasaurid taxonomic richness saw a  
51 steep increase (Polcyn et al. 2014), with speciation in the Western Interior Seaway (WIS) in central North  
52 America triggering a diversification during the so-called ‘Niobraran Age’ (e.g. Kiernan 2002; Russell 1967).  
53 High taxonomic richness persisted through the mid-Campanian (e.g. Driscoll et al. 2019), where an abrupt  
54 taxonomic turnover is observed in central North America at the onset of the ‘Navesinkan Age’ (e.g. Russell  
55 1993; Kiernan 2002). The abrupt shift observed in WIS mosasaurid community is mirrored in northern Europe  
56 (Lindgren 2004), Japan (Tanimoto 2005; Sato et al. 2012), South America (Jiménez-Huidobro, Simões, and  
57 Caldwell 2017), and to some extent in Oceania (Jiménez-Huidobro, Simões, and Caldwell 2017). Mosasaurids  
58 seem to maintain a high diversity throughout the Maastrichtian, yet with varying assemblages (Cappetta et al.  
59 2014). Despite abundant remains, it is unknown whether these changes in taxonomic composition resulted in  
60 constriction of functional or ecomorphological variation of these top oceanic predators on provincial or global  
61 scales leading up to the end-Cretaceous mass extinction.

62

63 For the first time, we explore global mosasaurid ecomorphological variation throughout the final chapter of  
64 the Mesozoic (84–66 Mya) at both local and global scales, using a set of cranial and postcranial  
65 measurements, including data from several tens of high-precision 3D models. Because of the strong  
66 conservative forces governing mosasaurid bauplan evolution (e.g. hydrodynamic performance and phyletic  
67 heritage; e.g. Stubbs and Benton 2016), we did not anticipate significant temporal changes in craniodental  
68 morphofunctional disparity. Yet, we demonstrate polarisation of ecomorphospace occupation and significant  
69 drops in mosasaur disparity just before the K/Pg mass extinction, most notably in the Northern Hemisphere.

70

## 71 **MATERIAL AND METHODS**

### 72 **Taxonomic and Morphological Sampling**

73 Skull and jaw material from 93 mosasaurid specimens were collected, representing 56 species and all  
74 subfamilies and tribes (Polcyn et al. 2014; Simões et al. 2017). The taxonomic composition of mosasaurid  
75 clades in this study follows the results of Simões et al. (2017); we consider halisaurines as basal mosasaurids,  
76 and treat Russellosaurina (including Tethysaurinae, Tylosaurinae, Plioplatecarpinae, and Yaguarasaurinae)  
77 and Mosasaurina (including Mosasaurinae) as monophyletic groups. Morphometric information was collected  
78 from two main sources: three-dimensional laser and structured light surface scans as well as photogrammetric  
79 models were the preferred methodology, supplemented with two-dimensional published images and first-hand  
80 photographs. Laser scanned specimens were digitised using a Creafom HandySCAN 300 handheld laser  
81 scanner at resolution 0.2–0.5mm; structured light scanning was performed using an Artec Eva handheld  
82 scanner, at resolution 0.5mm; photogrammed models were captured using a Nikon D3000 DSLR camera  
83 (burst mode with light-ring), with 3D models generated using Agisoft Metashape 1.6.3., scaled in MeshLab  
84 2020.06 (Cignoni et al. 2008). All specimens are listed in Supplementary Information 1: Specimen List; 3D  
85 models will be provided in the open-source repository MorphoSource on peer-reviewed acceptance.

86

### 87 **Linear Measurements and Functional Ratios**

88 Twenty-four linear measurements were taken across the entire skull including dentition (Figure 1). Linear  
89 measurements on 3D scans were taken using the measurement tool in MeshLab 2020.06; measurements on 2D  
90 images were performed using the line measuring tool in ImageJ (Schneider, Rasband, and Eliceiri 2012).  
91 These measurements were then used to generate 16 functional ratios describing the craniodental architecture  
92 (Table 1). All these traits have clearly established functional importance or outcomes (Figure 1; for further  
93 details, see Supplementary Information 2: Functional Ratios). Examples include the ratio of mandibular lever  
94 arms (proxies for mechanical advantage, i.e. ratio of muscular input force to output force on prey items),

95 supratemporal fenestrae area (proxy for cross-sectional area of combined jaw adductor musculature), and  
96 relative orbit size (amount of the skull dedicated to housing the eyeball).

97 A threshold of 40% trait completeness was applied to the sample, on each specimen; percentages of missing  
98 data per species can be found in Supplementary Information 3: Species Coverage. A resultant craniodental  
99 dataset with all 16 functional ratios was subjected to the 40% threshold. Following the threshold  
100 computations, 18.2% of missing trait data was recorded, and the dataset included all 58 taxa studied. Trait  
101 ratios were standardised using a z-transformation to assign all characters a mean of 0 and a variance of 1; data  
102 which cleared the 40% completeness threshold were used to compute a Euclidean distance matrix for  
103 ordination analyses and disparity calculation.

104

## 105 **Ecomorphospaces**

106 Ordination of trait data was visualised in two-dimensions in two ways: a principal coordinates analysis  
107 (PCoA) and a non-metric multidimensional scaling approach (NMDS). PCoAs were performed using a  
108 cailliez correction criterion to correct for negative eigenvalues (using ape v.5.3; Paradis, Claude, and  
109 Strimmer 2004), and were preferred to principal components analysis (PCA) as PCoA allows missing values  
110 in the Euclidean distance matrix. Comparisons between PCoA and non-metric multidimensional scaling  
111 (NMDS) ordination demonstrated comparable patterns of ecomorphospace occupation. NMDS are used for  
112 visualisation here as they pack more variation of the data into a two-dimensional graph. However, as NMDS  
113 axes are not ideal to use as variables for disparity analyses because of their non-metric properties, all PCoA  
114 axes were chosen for assessment of morphofunctional disparity in through time, within clades, and across  
115 geographic regions. Comparative NMDS analyses were performed in ‘vegan’ v.2.5-6 (Oksanen et al. 2018);  
116 graphical results from PCoA ecomorphospaces can be found in Supplementary Figure S1. Kernel 2D density  
117 estimates were used to visualise density-based macroevolutionary landscapes, plotted onto NMDS  
118 ecomorphospaces, following the methodology of Fischer et al. (2020). Moreover, mandible length (proxy for  
119 body size) was used both in scaling datapoints to visually inspect the spread of large-sized mosasaurids, and  
120 additionally to compare the spread of body sizes in mosasaurids through the Campanian-Maastrichtian.

121

## 122 **Disparity**

123 Morphofunctional disparity was calculated based on PCo axes. In addition, mosasaurid communities from  
124 four geographically distinct regions were investigated: the Western Interior Seaway (WIS); Northern Tethys  
125 Province (NTP); Southern Tethys Province (STP; Bardet 2012); and Weddellian Province (consisting of  
126 South-East Oceania, the Antarctic peninsula and Patagonia; WP). Disparity was measured through time,  
127 focusing on time bins bearing mosasaurid fossils during the latest Cretaceous: Early Campanian (83.60–77.85  
128 Mya); Late Campanian (77.85–72.10 Mya); Early Maastrichtian (72.10–69.05 Mya); Late Maastrichtian  
129 (69.05–65.50 Mya). The focus was made on these time periods as they encompassed the mosasaurid  
130 taxonomic turnover in the mid-Campanian, and enabled the investigation of disparity in the lead up to the end-  
131 Cretaceous mass extinction. Total disparity within mosasaurid clades and geographic regions during these  
132 time periods was also calculated. Disparity analyses were performed in RStudio using the *disparRity* package  
133 (v.1.5.0) (Guillerme 2018). The sum of variances (SoV) disparity metric was preferred, as it demonstrates  
134 robusticity to sample size variation between time bins (Ciampaglio, Kemp, and McShea 2009). Alternative  
135 disparity metrics (pairwise dissimilarity, PD; sum of ranges, SoR) were also tested to corroborate patterns  
136 observed using SoV metric (Supplementary Table S1). Bootstrap iterations were set at 1000 repetitions;  
137 additional bootstrapping procedures were performed to account for false positive results when testing for  
138 significant differences (see Supplementary Table S1). Here, we adapt the terminology from population  
139 ecology to assess disparity at the regional level (here termed ‘ $\alpha$ -disparity’) and global level (‘ $\gamma$ -disparity’). In  
140 order to examine how mosasaurid ecomorphological disparity was differentiated across regional communities,  
141  $\gamma$ -disparity per time bin was divided by mean  $\alpha$ -disparity across all provinces per time bin (following  
142 population ecology methods e.g. Legendre 2008), creating ‘ $\beta$ -disparity’. Beta-disparity can be defined as a  
143 measure of disparity differentiation; a high  $\beta$ -disparity indicates a greater range of mean  $\alpha$ -disparity values  
144 within a specific time-bin, whereas low  $\beta$ -disparity indicates more uniformity in mean  $\alpha$ -disparity values,  
145 suggesting less ecomorphological differentiation between disparities across communities. Mean bootstrap  
146 estimates (1000 replications) were used as metrics for  $\alpha$ - and  $\gamma$ -disparity calculations, and compared through  
147 four time-bins (Early Campanian; Late Campanian; Early Maastrichtian; Late Maastrichtian). Changes in

148 disparity between subsequent time bins and between clades/geographic regions were tested for using non-  
149 parametric Wilcoxon tests in the ‘stats’ package (v.4.0.3) (R Core Development Team 2008), with Bonferroni  
150 corrections for multiple comparisons.

151

## 152 **RESULTS**

### 153 **Morphospace occupation**

154 We quantified mosasaurid craniodental disparity across the Campanian-Maastrichtian interval. Our aims were  
155 to establish whether faunal transitions yielded changes in disparity in mosasaurids as well as whether global  
156 and provincial mosasaurid disparity was in decline prior to the end-Cretaceous mass extinction. Most notably,  
157 large ‘megapredatory’ taxa with cutting dentition, including almost all tylosaurines (Figure 2A; filled purple  
158 squares), and the majority of large mosasaurines cluster in the ecomorphospace (Figure 2A). These results  
159 suggest that overall skull functional morphology within these two (occasionally contemporaneous) clades of  
160 megapredatory marine reptiles converged, despite numerous phylogenetic differences. A number of  
161 brevirostrine mosasaurines occupy regions of positive NMDS axis 1, typified by relatively large  
162 supratemporal fenestrae, deep jaws, blunt rostra and crushing dentition (e.g. *Globidens* spp.). The upper half  
163 of ecomorphospace (positive values along NMDS axis 2) is occupied predominantly by primitive mosasaurids  
164 (halisaurines, tethysaurines) and *Plioplatecarpus* spp., which all had large orbits, gracile skulls, and recurved,  
165 piercing teeth (Figure 2A; see also Supplementary Figure S1); they constitute our ‘grasping’ cluster (Figure  
166 2A & 2E).

167

168 The density of ecomorphospace occupation through time (Figure 2B-E) reveals a series of changes across the  
169 Campanian-Maastrichtian interval. Many mosasaurines and rüsselosaurines occupy a large ‘megapredatory’  
170 region through the Early Campanian to the Early Maastrichtian. The majority of rüsselosaurines disappear  
171 afterwards, strongly altering the pattern of ecomorphospace occupation (Figure 2E) by creating a clear divide  
172 between two main clusters in the late Maastrichtian bin: the ‘megapredatory’ cluster, formed predominantly  
173 by *Tylosaurus* and *Mosasaurus* and the ‘grasping’ cluster, formed by *Plioplatecarpus*, halisaurines, and the

174 Weddellian taxa *Taniwhasaurus oweni* and *Rikisaurus tehoensis*. In addition to this polarisation of mosasaurid  
175 craniodental shape, a few taxa also evolved longirostrine (e.g. *Gavialimimus*) and brevirostrine (likely  
176 durophagous; e.g. *Globidens* spp.) morphologies (Figures 2A-B). Our analyses of clade disparity add support  
177 to the ecomorphospace signal, with decreases in tylosaurine, plioplatecarpine, and plotosaurin disparity  
178 through the Maastrichtian (Supplementary Figure S2).

179

### 180 **Evolution of skull size**

181 Changes in mosasaurid communities also resulted in slight variation in skull size distributions (proxy for body  
182 size) across the Campanian – Maastrichtian interval (Figure 2F). Early Campanian size distribution is notably  
183 more uniform, with comparable densities of large and small mosasaurids (Figure 2F; blue line). By  
184 comparison, density of smaller species is lower in the Late Maastrichtian, leading to a peak in mid-sized and  
185 very large species (Figure 2F; yellow line). This pattern tracks the presence of multiple very large late  
186 Maastrichtian tylosaurines and plotosaurins (a pattern mirrored in sharks; Cappetta et al. 2014), and highlights  
187 the extinction of smaller species which were abundant during the Campanian (e.g. *Clidastes*,  
188 *Plesioplatecarpus*) (Figure 2B-C). However, these differences are not significant, indicating that the changes  
189 in ecomorphospace occupation and disparity we observe are not associated with strong changes in mosasaurid  
190 size, but rather with the functional capacities of their skulls.

191

### 192 **Spatiotemporal evolution of disparity**

193 We find a significant increase in global ( $\gamma$ ) ecomorphological disparity in mosasaurids (Figure 3A) coincident  
194 with taxonomic turnovers known to have occurred at the mid-Campanian boundary (the ‘Niobraran-  
195 Navesinkan’ transition; Lindgren 2004; Tanimoto 2005; Sato et al. 2012; Jiménez-Huidobro, Simões, and  
196 Caldwell 2017; Kiernan 2002; Russell 1993). The observed increase in  $\gamma$ -disparity is common across all  
197 disparity metrics we computed (sum of variances, sum of ranges, pairwise dissimilarity; Supplementary Table  
198 S3). Our results demonstrate that  $\gamma$ -disparity of mosasaurid ecomorphologies increased from Early to Late  
199 Campanian and continued increasing until the Early Maastrichtian, mirroring the expansion of the



200 craniodental ecomorphospace occupation (Figure 2B-D). Mosasaurid diversity (in this sample) somewhat  
201 tracks fluctuations in disparity, but not to the same magnitude (Figure 3). By the Late Maastrichtian,  $\gamma$ -  
202 disparity is higher than that recorded throughout the Campanian, despite fewer species being present in the  
203 Late Maastrichtian (Figure 3A; Table 2).

204

205 While disparity increases on global ( $\gamma$ ) and provincial ( $\alpha$ ) scales from the Campanian to the Maastrichtian  
206 (Table 2), we observe significant declines in  $\gamma$ -disparity from early to late-Maastrichtian leading up to the K-  
207 Pg mass extinction (Figure 3A-E). When examined at the provincial level (Figure 3B-E), the early-late  
208 Maastrichtian transition records declines in  $\alpha$ -disparity for all provinces (with the exception of STP; Table 2)  
209 using almost all disparity metrics, reinforcing the global outlook of a significant decline in ecomorphological  
210 disparity in mosasaurids in the latest Maastrichtian. This disparity decrease is found within all well-sampled  
211 clades as well, no matter the disparity metric used, with the exception the pairwise dissimilarity metric which  
212 slightly increased for the hyper-disparate group Globidensini through the Maastrichtian (Figure 2D-E). Sharp  
213 decreases in tylosaurine and plioplatecarpine presence in the Western Interior Seaway contribute to the  
214 decline in  $\alpha$ -disparity in this region; by contrast, the presence of highly disparate globidensins in the Southern  
215 Tethys Province contributes toward more stable overall  $\gamma$ -disparity during the Maastrichtian (Figure 3A &  
216 3D). Differentiation of disparity across regions (i.e.  $\beta$ -disparity) increases from early to late Maastrichtian  
217 (Table 2); this increase in  $\beta$ -disparity can be attributed to several factors: decreases in  $\alpha$ -disparity in several  
218 (but crucially, not all) observed provinces; reductions in taxon count (Figure 3B-E); decreased occupancy of  
219 previously commonly exploited niches (e.g. reduction of ‘megapredators’; Figure 2E); and increased  
220 endemism (e.g. Moroccan fauna of the STP; Strong et al. 2020; Lingham-Soliar 2002; Leblanc, Mohr, and  
221 Caldwell 2019; Longrich, Bardet, Khaldoune, et al. 2021; Longrich, Bardet, Schulp, et al. 2021).

222

## 223 **DISCUSSION**

### 224 **The necessity for regional and global assessments of pre-extinction diversity and disparity**

225 The influence of localised faunal assemblages in the fossil record is well known to affect global patterns  
226 diversity and disparity (i.e. Close et al. 2019; Upchurch et al. 2011; Condamine et al. 2021; etc.). For many  
227 groups of large tetrapods, the global fossil record is not well resolved, whereas regional sampling in certain  
228 geographic areas is strong, and consequent global biodiversity/disparity estimates can be heavily reliant on  
229 those few regions (e.g. Brusatte et al. 2012; Sax and Gaines 2003; Benson et al. 2010; Cleary et al. 2015; etc.).  
230 In many studies, including ours, it is clear that the sampling effort in North America over the past 150 years is  
231 an important factor in estimating pre-Maastrichtian tetrapod diversity and disparity (e.g. Maidment et al. 2021;  
232 Vavrek and Larsson 2010; Longrich, Scriberas, and Wills 2016). Regional diversity patterns are thus likely to  
233 contain an important signal, as the highly-fragmented world of the Mesozoic and Cenozoic likely resulted in  
234 ecosystems with distinct compositions and physico-chemical parameters (Zaffos, Finnegan, and Peters 2017).  
235 This reality has often been overlooked when analysing tetrapod diversity and disparity patterns leading up to  
236 and across the K/Pg mass extinction. Indeed, a series of studies on the extinction of non-avian dinosaurs have  
237 recovered conflicting results (Brusatte et al. 2012; Condamine et al. 2021; Maidment et al. 2021; Dean,  
238 Chiarenza, and Maidment 2020; Chiarenza et al. 2019; Vavrek and Larsson 2010), notably because of their  
239 varying treatment of regional differences and their sampling.

240

241 Even though the fossil record of mosasaurids appears only weakly biased (Driscoll et al. 2019), and marine  
242 reptile sampling indicators are generally excellent for the Campanian-Maastrichtian interval (Fischer et al.  
243 2016), our results clearly indicate regional variations in the ecomorphological disparity patterns of  
244 mosasaurids. The drivers of these differences should not necessarily be regarded as global; a telling example  
245 are the provincial disparity patterns during the Maastrichtian (Figure 3B-E), which may be associated with the  
246 magnitude of the environmental changes resulting from the sea level regressions. Indeed, the epicontinental  
247 WIS greatly changed in extent and shape during the Maastrichtian (Berry 2017; Slattery et al. 2013), and this  
248 region records the steepest decrease in  $\alpha$ -disparity, while deeper basins such as Northern and Southern Tethys  
249 Provinces were seemingly less affected (Bardet et al. 2014; Hornung, Reich, and Frerichs 2018; Lindgren  
250 2004; Bardet 2012). In this context, focussing on the abundant North American record to reconstruct the  
251 global diversity or disparity patterns of mosasaurids would result in a steeper late Maastrichtian decrease than

252 that which was computed for other regions, hence confounding regional and global factors at play prior to the  
253 K/Pg mass extinction.

254

### 255 **Pre-K/Pg mosasaurid turnovers and crises**

256 The ‘Niobraran-Navesinkan’ (Early to Late Campanian) taxonomic transition from russellosaurine-to-  
257 mosasaurine-dominated communities was initially identified in the Western Interior Seaway (WIS) (e.g.  
258 Russell 1993), with similar turnovers identified in multiple other regions across the globe (Lindgren 2004;  
259 Tanimoto 2005; Sato et al. 2012; Jiménez-Huidobro, Simões, and Caldwell 2017). We show that, far from  
260 experiencing a global  $\gamma$ -disparity decline during this turnover, mosasaurids significantly increased in disparity  
261 across this transition. However, this is in no small part due to the extinction of more ‘generalist’ and small-  
262 sized plioplatecarpines and tylosaurines (Figure 3A). These extinctions in the WIS reduced the density of  
263 ‘megapredatory’ and ‘generalist’ ecomorphologies in the Late Campanian bin (Figure 2B-C), causing  
264 increased polarisation of the remaining ecomorphologies exhibited by mosasaurid taxa. The removal of  
265 common morphologies from a sample can impact disparity as much as the inclusion of highly disparate forms;  
266 this is the case for a series of disparity metrics (but obviously not the sum of ranges). We observe this pattern  
267 for mosasaurid  $\gamma$ -disparity through the Campanian (Figure 2B-C; Figure 3A). Actually, the increase in  
268 morphofunctional disparity at the ‘Niobraran-Navesinkan’ transition is a phenomenon local to the Western  
269 Interior Seaway, with a high enough amplitude to influence global patterns; other regions maintain stable  
270 morphofunctional disparity through this interval (Figure 3; Table 2). The cause behind the abrupt shift in  
271 mosasaurid community composition across the ‘Niobraran-Navesinkan’ is as yet unclear. A decrease in  
272 oceanic temperature between the mid- and late-Campanian is coincident with the turnover (Polcyn et al. 2014;  
273 Linnert et al. 2016), which essentially removed smaller species within multiple clades (e.g. *Selmasaurus*,  
274 *Plesioplatecarpus*, *Tylosaurus kansasensis*). This seemingly selective extinction suggests that body size was  
275 an important factor in lineage survival across this local event (Figure 2B-C and 2F). By contrast, mosasaurid  
276 assemblages from the Campanian elsewhere do not suggest clear reductions in smaller species at the mid-  
277 Campanian boundary (Lindgren 2004; Jagt 2005), nor do they exhibit a radical shift in  $\alpha$ -disparity (Table 2).

278

279 Later, a decrease in global  $\gamma$ -disparity and  $\alpha$ -disparity is found within the Maastrichtian, in nearly all regions  
280 and across all clades. When the differentiation of ecomorphological disparity between geographical regions is  
281 considered (i.e.  $\beta$ -disparity; Table 2), it is clear that the Late Maastrichtian was a time of increased  
282 regionalisation of mosasaurid disparity, rather than a consistent global decline. Communities of mosasaurids  
283 in the WIS, NTP and WP are shown to be notably more homogeneous in the Late Maastrichtian than those of  
284 the Early Maastrichtian (Figure 3B-E), with the WIS and WP communities represented by very few taxa  
285 within only two tribes (Plotosaurini+Globidensini, and Plotoaurini+Tylosaurini respectively). By contrast, the  
286 Late Maastrichtian mosasaurid community of the STP was comprised of a ecomorphologically diverse  
287 assemblage of globidensins (e.g. *Globidens*), plotosaurins (*Mosasaurus* spp.), halisaurines (e.g. *Pluridens*),  
288 and plioplatecarpines (e.g. *Gavialimimus*) (Strong et al. 2020; Leblanc, Caldwell, and Bardet 2012; Bardet et  
289 al. 2004; Longrich, Bardet, Schulp, et al. 2021), yielding a high  $\alpha$ -disparity in this region (Figure 3D). The  
290 retention of disparate ecomorphologies of STP mosasaurids through the Maastrichtian drives the spike in  $\beta$ -  
291 disparity observed in the Late Maastrichtian (Table 2), representing a peak in provincial differentiation. The  
292 predominantly bimodal landscape of mosasaurids in the late Maastrichtian (Figure 2E) suggests that, while a  
293 variety of niches were still being occupied by low densities of disparate mosasaurids, numerous Northern and  
294 Southern Tethys mosasaurids exhibited ‘megapredatory’ or ‘grasping’ functional adaptations (Figure 2; also  
295 Bardet 2012; Lindgren 2004; Bardet et al. 2014). Becoming increasingly apparent is the importance of the  
296 Southern Tethys Province (including Afro-Arabia, Morocco, Niger-Nigeria, Angola and eastern Brazil) in  
297 estimating late-Maastrichtian marine reptile diversity and disparity (e.g. Strong et al. 2020; Leblanc, Mohr,  
298 and Caldwell 2019; Longrich, Bardet, Schulp, et al. 2021; Longrich, Bardet, Khaldoune, et al. 2021).

299 Understanding patterns such as these are vital for the accurate interpretation of faunal dynamics and functional  
300 variation before and after extinction events. If only  $\gamma$ -disparity of mosasaurids were considered, then this  
301 group could be interpreted as being in decline prior to their ultimate demise at the K/Pg boundary. However, it  
302 is apparent that when both  $\alpha$ - and  $\beta$ -disparities are taken into account, some regional communities were most  
303 certainly declining in taxonomic diversity and ecomorphological disparity, whereas others were only  
304 minimally affected on both counts.

305

306 **How selective are the pre-K/Pg extinctions in marine reptiles?**

307 The Early Maastrichtian is identified here as the time of greatest  $\gamma$ -disparity of mosasaurids (Figure 3A), with  
308 expansion of ecomorphospace occupation by longirostrine and brevirostrine ecomorphologies, in addition to  
309 an increase in halisaurine and plioplatecarpine species occupying new regions of ecomorphospace in the  
310 ‘grasping’ cluster (Figure 2A+D). This Early Maastrichtian rise in disparity appears to be driven by multiple  
311 originations in the two Tethys Provinces (North and South). With regards to other marine reptile fauna,  
312 ichthyosaurians and pliosaurids were long gone by the Late Maastrichtian (Schumacher 2011; Fischer et al.  
313 2016; Bardet 1994), and the predominant marine reptiles in the Campanian-Maastrichtian were restricted to  
314 xenopsarian plesiosaurians, mosasaurids, chelonoids, and crocodylians (e.g. Bardet et al. 2014). These clades  
315 do not seem to follow a disparity pattern similar to that recovered here for mosasaurids. For example,  
316 polycotyloid plesiosaurians were already in decline in both phylogenetic diversity and ecomorphological  
317 disparity during the Campanian-Maastrichtian interval (Fischer et al. 2018), with only the polycotyline  
318 *Dolichorhynchops herschelensis* and the occultonecian *Sulcusuchus erraini* potentially being present during  
319 the Maastrichtian (in addition to a handful of indeterminate remains; Sato 2005; Kaddumi 2006; O’gorman  
320 and Gasparini 2013; Fischer et al. 2018). Robust evaluations of elasmosaurid disparity are still lacking, but the  
321 range of phenotypes (either in terms of phylogenetic diversity, osteology or relative neck length) appears to  
322 still be broad during the Maastrichtian, although within-Maastrichtian changes have not yet been computed  
323 (Fischer et al. 2021). Similarly, within-Maastrichtian disparity dynamics have not been explored for marine  
324 testudines, although previous assessments of testudines indicate a peak in cranial morphological variation in  
325 the Maastrichtian (Foth and Joyce 2016; Foth, Ascarrunz, and Joyce 2017), and a consistent contribution to  
326 the diversity of feeding morphologies across marine reptiles from Campanian to Maastrichtian (Stubbs and  
327 Benton 2016). By contrast, aquatic crocodyliformes exhibit comparatively low disparity in the latest  
328 Cretaceous. Dramatic declines in marine crocodyliform morphological disparity are known to have occurred  
329 from Jurassic to Cretaceous, which potentially left niches open for mosasaurids to exploit during their own  
330 radiation in the Cenomanian (Stubbs et al. 2013; Stubbs and Benton 2016). Subsequently, crocodyliform  
331 morphological disparity was in decline throughout the late Cretaceous (Wilberg 2017; Stubbs et al. 2021); the

332 exception to this pattern were the aquatic dyrosaurid tethysuchians, which exhibited a rapid burst of  
333 morphological evolution in the Maastrichtian (Stubbs et al. 2021), coinciding with increased regionalisation of  
334 mosasaurid ecomorphological disparity revealed in this study. The increased endemism and expansion into  
335 ‘grasping’ and ‘longirostrine’ ecomorphologies by mosasaurids in the Late Maastrichtian combines with  
336 isotopic analyses of trophic structure in the Maastrichtian of the Southern Tethys Province (Martin et al.  
337 2017), suggesting increased dietary specialisation, as multiple predators coexisted and often fed upon prey  
338 from a single trophic level . Patterns of taxonomic diversity and ecomorphological disparity across multiple  
339 marine reptile groups indicate that wholesale (and in some cases fragile) restructuring of marine trophic webs  
340 was underway before the K-Pg mass extinction event.

341

#### 342 **Acknowledgements**

343 The authors would like to thank the museum curators for access to their specimens for photographing and  
344 scanning: Megan Sims, Anna Whitaker, and Chris Beard (KUVP, Kansas); Chase Shelburne and Laura  
345 Wilson (FHSM, Kansas); Amanda Millhouse and Matt Miller (USNM, Washington DC); Amy Henrici  
346 (CMNH, Pittsburgh); Bill Simpson (FMNH, Chicago); Laura Vietti (UW, Laramie); Jodee Reed (FFHM,  
347 Oakley); Annelise Folie (RBINS, Brussels); Ronan Allain (MNHN, Paris); Benjamin Kear (PMU, Uppsala).  
348 We also thank Mike Polcyn for access to 3D data from published articles. This work was funded by grants  
349 from the Fonds De La Recherche Scientifique (F.R.S.-FNRS): MIS F.4511.19 “SEASCAPE” (VF), FNRS  
350 travel grant 35706165 (JAM), and a FRIA doctoral fellowship (RFB).

351

#### 352 **Author Contributions**

353 JAM and VF conceived the study. JAM, RFB, and VF collected raw data. JAM and VF conducted statistical  
354 analyses and designed figures. JAM, NB, and VF wrote the manuscript. All authors contributed to the final  
355 manuscript.

356

357 **References**

- 358 Bardet, Nathalie. 1994. "Extinction Events Among Mesozoic Marine Reptiles." *Historical Biology* 7 (4): 313–  
359 24. <https://doi.org/10.1080/10292389409380462>.
- 360 ———. 2012. "Maastrichtian Marine Reptiles of the Mediterranean Tethys: A Palaeobiogeographical  
361 Approach." *Bulletin de La Societe Geologique de France* 183 (6): 573–96.  
362 <https://doi.org/10.2113/gssgfbull.183.6.573>.
- 363 Bardet, Nathalie, Alexandra Houssaye, Peggy Vincent, Xabier Pereda Suberbiola, Mbarek Amaghazaz, Essaid  
364 Jourani, and Saïd Meslouh. 2014. "Mosasaurids (Squamata) from the Maastrichtian Phosphates of  
365 Morocco: Biodiversity, Palaeobiogeography and Palaeoecology Based on Tooth Morphoguilds."  
366 *Gondwana Research* 27 (3): 1068–78. <https://doi.org/10.1016/j.gr.2014.08.014>.
- 367 Bardet, Nathalie, Xabier Pereda Suberbiola, Mohamed Iarochene, Fatima Bouyahyaoui, Baadi Bouya, and  
368 Mbarek Amaghazaz. 2004. "*Mosasaurus Beaugei* Arambourg, 1952 (Squamata, Mosasauridae) from the  
369 Late Cretaceous Phosphates of Morocco." *Geobios* 37 (3): 315–24.  
370 <https://doi.org/10.1016/j.geobios.2003.02.006>.
- 371 Benson, Roger B. J., Richard J. Butler, Johan Lindgren, and Adam S. Smith. 2010. "Mesozoic Marine  
372 Tetrapod Diversity: Mass Extinctions and Temporal Heterogeneity in Geological Megabiases Affecting  
373 Vertebrates." *Proceedings of the Royal Society B: Biological Sciences* 277 (1683): 829–34.  
374 <https://doi.org/10.1098/RSPB.2009.1845>.
- 375 Berry, Keith. 2017. "New Paleontological Constraints on the Paleogeography of the Western Interior Seaway  
376 near the End of the Cretaceous (Late Campanian–Maastrichtian) with a Special Emphasis on the  
377 Paleogeography of Southern Colorado, U.S.A." *Rocky Mountain Geology* 52 (1): 1–16.  
378 <https://doi.org/10.24872/RMGJOURNAL.52.1.1>.
- 379 Brusatte, Stephen L., Richard J. Butler, Albert Prieto-Márquez, and Mark A. Norell. 2012. "Dinosaur  
380 Morphological Diversity and the End-Cretaceous Extinction." *Nature Communications* 2012 3:1 3 (1):  
381 1–8. <https://doi.org/10.1038/ncomms1815>.

- 382 Butler, Richard J., Stephen L. Brusatte, Brian Andres, and Roger B. J. Benson. 2012. “How Do Geological  
383 Sampling Biases Affect Studies of Morphological Evolution in Deep Time? A Case Study of Pterosaur  
384 (Reptilia: Archosauria) Disparity.” *Evolution* 66 (1): 147–62. [https://doi.org/10.1111/j.1558-  
385 5646.2011.01415.x](https://doi.org/10.1111/j.1558-5646.2011.01415.x).
- 386 Cappetta, Henri, Nathalie Bardet, Xabier Pereda Suberbiola, Sylvain Adnet, Driss Akkrim, Mohamed Amalik,  
387 and Aziza Benabdallah. 2014. “Marine Vertebrate Faunas from the Maastrichtian Phosphates of  
388 Benguérir (Ganntour Basin, Morocco): Biostratigraphy, Palaeobiogeography and Palaeoecology.”  
389 *Palaeogeography, Palaeoclimatology, Palaeoecology* 409: 217–38.  
390 <https://doi.org/10.1016/j.palaeo.2014.04.020>.
- 391 Chiarenza, Alfio Alessandro, Philip D. Mannion, Daniel J. Lunt, Alex Farnsworth, Lewis A. Jones, Sarah-  
392 Jane Kelland, and Peter A. Allison. 2019. “Ecological Niche Modelling Does Not Support Climatically-  
393 Driven Dinosaur Diversity Decline before the Cretaceous/Paleogene Mass Extinction.” *Nature  
394 Communications* 2019 10:1 10 (1): 1–14. <https://doi.org/10.1038/s41467-019-08997-2>.
- 395 Ciampaglio, Charles N., Matthieu Kemp, and Daniel W. McShea. 2009. “Detecting Changes in Morphospace  
396 Occupation Patterns in the Fossil Record: Characterization and Analysis of Measures of Disparity.”  
397 *Paleobiology* 27 (4): 695–715. [http://www.psjournals.org/doi/abs/10.1666/0094-  
398 8373%282001%29027%3C0695%3ADCIMOP%3E2.0.CO%3B2](http://www.psjournals.org/doi/abs/10.1666/0094-8373%282001%29027%3C0695%3ADCIMOP%3E2.0.CO%3B2).
- 399 Cignoni, P., M. Callieri, M. Corsini, M. Dellapiane, F. Ganovelli, and G. Ranzuglia. 2008. “MeshLab: An  
400 Open-Source Mesh Processing Tool.” In *Eurographics Italian Chapter Conference*, edited by V.  
401 Scarano, R. De Chiara, and U. Erra, 1–8. Salerno.
- 402 Cleary, Terri J., Benjamin C. Moon, Alexander M. Dunhill, and Michael J. Benton. 2015. “The Fossil Record  
403 of Ichthyosaurs, Completeness Metrics and Sampling Biases.” *Palaeontology* 58 (3): 521–36.  
404 <https://doi.org/10.1111/PALA.12158>.
- 405 Close, Roger A., Roger B. J. Benson, John Alroy, Anna K. Behrensmeyer, Juan Benito, Matthew T. Carrano,  
406 Terri J. Cleary, et al. 2019. “Diversity Dynamics of Phanerozoic Terrestrial Tetrapods at the Local-  
407 Community Scale.” *Nature Ecology & Evolution* 2019 3:4 3 (4): 590–97.



- 408 <https://doi.org/10.1038/s41559-019-0811-8>.
- 409 Condamine, Fabien L., Guillaume Guinot, Michael J. Benton, and Philip J. Currie. 2021. “Dinosaur  
410 Biodiversity Declined Well before the Asteroid Impact, Influenced by Ecological and Environmental  
411 Pressures.” *Nature Communications* 2021 12:1 12 (1): 1–16. [https://doi.org/10.1038/s41467-021-23754-](https://doi.org/10.1038/s41467-021-23754-0)  
412 0.
- 413 Dean, Christopher D., A. Alessandro Chiarenza, and Susannah C. R. Maidment. 2020. “Formation Binning: A  
414 New Method for Increased Temporal Resolution in Regional Studies, Applied to the Late Cretaceous  
415 Dinosaur Fossil Record of North America.” *Palaeontology* 63 (6): 881–901.  
416 <https://doi.org/10.1111/PALA.12492>.
- 417 Driscoll, Daniel A., Alexander M. Dunhill, Thomas L. Stubbs, and Michael J. Benton. 2019. “The Mosasaur  
418 Fossil Record through the Lens of Fossil Completeness.” *Palaeontology* 62 (1): 51–75.  
419 <https://doi.org/10.1111/pala.12381>.
- 420 Fischer, Valentin, Nathalie Bardet, Roger B. J. Benson, Maxim S. Arkhangelsky, and Matt Friedman. 2016.  
421 “Extinction of Fish-Shaped Marine Reptiles Associated with Reduced Evolutionary Rates and Global  
422 Environmental Volatility.” *Nature Communications* 2016 7:1 7 (1): 1–11.  
423 <https://doi.org/10.1038/ncomms10825>.
- 424 Fischer, Valentin, Roger B. J. Benson, Patrick S. Druckenmiller, H. F. Ketchum, and Nathalie Bardet. 2018.  
425 “The Evolutionary History of Polycotyloid Plesiosaurians.” *Royal Society Open Science* 5 (3).  
426 <https://doi.org/10.1098/RSOS.172177>.
- 427 Fischer, Valentin, Roger B.J. Benson, Nikolay G. Zverkov, Laura C. Soul, Maxim S. Arkhangelsky, Olivier  
428 Lambert, Ilya M. Stenshin, Gleb N. Uspensky, and Patrick S. Druckenmiller. 2017. “Plasticity and  
429 Convergence in the Evolution of Short-Necked Plesiosaurs.” *Current Biology* 27 (11): 1667-1676.e3.  
430 <https://doi.org/10.1016/j.cub.2017.04.052>.
- 431 Fischer, Valentin, Jamie A. MacLaren, Laura C. Soul, Rebecca F. Bennion, Patrick S. Druckenmiller, and  
432 Roger B.J. Benson. 2020. “The Macroevolutionary Landscape of Short-Necked Plesiosaurians.”

- 433 *Scientific Reports* 10 (1): 16434. <https://doi.org/10.1038/s41598-020-73413-5>.
- 434 Fischer, Valentin, Nikolay G Zverkov, Maxim S Arkhangelsky, Ilya M Stenshin, Ivan V Blagovetshensky,  
435 and Gleb N Uspensky. 2021. “A New Elasmosaurid Plesiosaurian from the Early Cretaceous of Russia  
436 Marks an Early Attempt at Neck Elongation.” *Zoological Journal of the Linnean Society* 192 (4): 1167–  
437 94. <https://doi.org/10.1093/ZOOLINNEAN/ZLAA103>.
- 438 Foth, Christian, Eduardo Ascarrunz, and Walter G. Joyce. 2017. “Still Slow, but Even Steadier: An Update on  
439 the Evolution of Turtle Cranial Disparity Interpolating Shapes along Branches.” *Royal Society Open  
440 Science* 4 (11). <https://doi.org/10.1098/RSOS.170899>.
- 441 Foth, Christian, and Walter G. Joyce. 2016. “Slow and Steady: The Evolution of Cranial Disparity in Fossil  
442 and Recent Turtles.” *Proceedings of the Royal Society B: Biological Sciences* 283 (1843).  
443 <https://doi.org/10.1098/RSPB.2016.1881>.
- 444 Guillerme, Thomas. 2018. “DispRity: A Modular R Package for Measuring Disparity.” Edited by Timothée  
445 Poisot. *Methods in Ecology and Evolution* 9 (7): 1755–63. <https://doi.org/10.1111/2041-210X.13022>.
- 446 Hornung, Jahn J., Mike Reich, and Udo Frerichs. 2018. “A Mosasaur Fauna (Squamata: Mosasauridae) from  
447 the Campanian (Upper Cretaceous).” *An Australasian Journal of Palaeontology* 42 (4): 543–59.  
448 <https://doi.org/10.1080/03115518.2018.1434899>.
- 449 Jagt, John W.M. 2005. “Stratigraphic Ranges of Mosasaurs in Belgium and the Netherlands (Late Cretaceous)  
450 and Cephalopod-Based Correlations with North America.” *Netherlands Journal of Geosciences /  
451 Geologie En Mijnbouw* 84 (3): 283–301. <https://doi.org/10.1017/S0016774600021065>.
- 452 Jiménez-Huidobro, Paulina, Tiago R. Simões, and Michael W. Caldwell. 2017. “Mosasauroids from  
453 Gondwanan Continents.” *Journal of Herpetology* 51 (3): 355–64. <https://doi.org/10.1670/16-017>.
- 454 Kaddumi, H. F. 2006. “A New Genus and Species of Gigantic Marine Turtles (Chelonioidea: Cheloniidae)  
455 from the Maastrichtian of the Harrana Fauna–Jordan.” *PalArch* 3 (1). [www.PalArch.nl](http://www.PalArch.nl).
- 456 Kiernan, Caitlin R. 2002. “Stratigraphic Distribution and Habitat Segregation of Mosasaurs in the Upper  
457 Cretaceous of Western and Central Alabama, with an Historical Review of Alabama Mosasaur

- 458 Discoveries.” *Journal of Vertebrate Paleontology* 22 (1): 91–103. <https://doi.org/10.1671/0272->  
459 4634(2002)022[0091:SDAHSO]2.0.CO;2.
- 460 Leblanc, Aaron R. H., Sydney R. Mohr, and Michael W. Caldwell. 2019. “Insights into the Anatomy and  
461 Functional Morphology of Durophagous Mosasaurines (Squamata: Mosasauridae) from a New Species  
462 of *Globidens* from Morocco.” *Zoological Journal of the Linnean Society* 186 (4): 1026–52.  
463 <https://doi.org/10.1093/zoolinnean/zlz008>.
- 464 Leblanc, Aaron R.H., Michael W. Caldwell, and Nathalie Bardet. 2012. “A New Mosasaurine from the  
465 Maastrichtian (Upper Cretaceous) Phosphates of Morocco and Its Implications for Mosasaurine  
466 Systematics.” *Journal of Vertebrate Paleontology* 32 (1): 82–104.  
467 <https://doi.org/10.1080/02724634.2012.624145>.
- 468 Legendre, Pierre. 2008. “Studying Beta Diversity: Ecological Variation Partitioning by Multiple Regression  
469 and Canonical Analysis.” *Journal of Plant Ecology* 1 (1): 3–8. <https://doi.org/10.1093/JPE/RTM001>.
- 470 Lindgren, Johan. 2004. “Stratigraphical Distribution of Campanian and Maastrichtian Mosasaurs in Sweden -  
471 Evidence of an Intercontinental Marine Extinction Event?” *GFF* 126 (2): 221–29.  
472 <https://doi.org/10.1080/11035890401262221>.
- 473 Lingham-Soliar, Theagarten. 2002. “First Occurrence of Premaxillary Caniniform Teeth in the Varanoidea:  
474 Presence in the Extinct Mosasaur *Goronyosaurus* (Squamata: Mosasauridae) and Its Functional and  
475 Paleocological Implications.” *Lethaia* 35 (2): 187–90. <https://doi.org/10.1080/002411602320184033>.
- 476 Linnert, Christian, Julia Engelke, Markus Wilmsen, and Jörg Mutterlose. 2016. “The Impact of the  
477 Maastrichtian Cooling on the Marine Nutrient Regime—Evidence from Midlatitudinal Calcareous  
478 Nannofossils.” *Paleoceanography* 31 (6): 694–714. <https://doi.org/10.1002/2015PA002916>.
- 479 Longrich, Nicholas R., Nathalie Bardet, Fatima Khaldoune, Oussama Khadiri Yazami, and Nour Eddine Jalil.  
480 2021. “*Pluridens Serpentis*, a New Mosasaurid (Mosasauridae: Halisaurinae) from the Maastrichtian of  
481 Morocco and Implications for Mosasaur Diversity.” *Cretaceous Research* 126 (October): 104882.  
482 <https://doi.org/10.1016/J.CRETRES.2021.104882>.

- 483 Longrich, Nicholas R., Nathalie Bardet, Anne S. Schulp, and Nour Eddine Jalil. 2021. “Xenodens  
484 Calminechari Gen. et Sp. Nov., a Bizarre Mosasaurid (Mosasauridae, Squamata) with Shark-like Cutting  
485 Teeth from the Upper Maastrichtian of Morocco, North Africa.” *Cretaceous Research* 123 (July):  
486 104764. <https://doi.org/10.1016/J.CRETRES.2021.104764>.
- 487 Longrich, Nicholas R., J. Scriberas, and M. A. Wills. 2016. “Severe Extinction and Rapid Recovery of  
488 Mammals across the Cretaceous–Palaeogene Boundary, and the Effects of Rarity on Patterns of  
489 Extinction and Recovery.” *Journal of Evolutionary Biology* 29 (8): 1495–1512.  
490 <https://doi.org/10.1111/JEB.12882>.
- 491 Maidment, Susannah C. R., Christopher D. Dean, Robert I. Mansergh, and Richard J. Butler. 2021. “Deep-  
492 Time Biodiversity Patterns and the Dinosaurian Fossil Record of the Late Cretaceous Western Interior,  
493 North America.” *Proceedings of the Royal Society B* 288 (1953).  
494 <https://doi.org/10.1098/RSPB.2021.0692>.
- 495 Martin, Jeremy E., Peggy Vincent, Théo Tacail, Fatima Khaldoune, Essaid Jourani, Nathalie Bardet, and  
496 Vincent Balter. 2017. “Calcium Isotopic Evidence for Vulnerable Marine Ecosystem Structure Prior to  
497 the K/Pg Extinction.” *Current Biology* 27 (11): 1641-1644.e2.  
498 <https://doi.org/10.1016/J.CUB.2017.04.043>.
- 499 Massare, Judy A. 1987. “Tooth Morphology and Prey Preference of Mesozoic Marine Reptiles.” *Journal of*  
500 *Vertebrate Paleontology* 7 (2): 121–37.
- 501 Motani, Ryosuke. 2002. “Swimming Speed Estimation of Extinct Marine Reptiles: Energetic Approach  
502 Revisited.” *Paleobiology* 28 (2): 251–62. [https://doi.org/10.1666/0094-](https://doi.org/10.1666/0094-8373(2002)028<0251:sseoem>2.0.co;2)  
503 [8373\(2002\)028<0251:sseoem>2.0.co;2](https://doi.org/10.1666/0094-8373(2002)028<0251:sseoem>2.0.co;2).
- 504 O’gorman, José P., and Zulma Gasparini. 2013. “Revision of *Sulcusuchus Erraini* (Sauropterygia,  
505 Polycotyliidae) from the Upper Cretaceous of Patagonia, Argentina.” *Alcheringa: An Australasian*  
506 *Journal of Palaeontology* 37 (2): 163–76. <https://doi.org/10.1080/03115518.2013.736788>.
- 507 Oksanen, Jari, F. Guillaume Blanchet, Michael Friendly, Roeland Kindt, Pierre Legendre, Dan McGlenn, Peter

- 508 R. Minchin, et al. 2018. “Vegan: Community Ecology Package.” [https://CRAN.R-](https://CRAN.R-project.org/package=vegan)  
509 [project.org/package=vegan](https://CRAN.R-project.org/package=vegan).
- 510 Paradis, Emmanuel, Julien Claude, and Korbinian Strimmer. 2004. “APE: Analyses of Phylogenetics and  
511 Evolution in R Language.” *Bioinformatics* 20 (2): 289–90.
- 512 Polcyn, Michael J., Louis L. Jacobs, Ricardo Araújo, Anne S. Schulp, and Octávio Mateus. 2014. “Physical  
513 Drivers of Mosasaur Evolution.” *Palaeogeography, Palaeoclimatology, Palaeoecology* 400: 17–27.  
514 <https://doi.org/10.1016/j.palaeo.2013.05.018>.
- 515 R Core Development Team. 2008. “R: A Language and Environment for Statistical Computing.” Vienna,  
516 Austria: R Foundation for Statistical Computing.
- 517 Russell, Dale A. 1967. *Systematics and Morphology of American Mosasaurs. Bulletin 23 of the Peabody*  
518 *Museum of Natural History Yale University*.
- 519 ———. 1993. “Vertebrates in the Western Interior Sea.” In *Evolution of the Western Interior Basin*, edited by  
520 W. G. E. Caldwell and E. G. Kaufmann, 665–680. Geological Association of Canada.
- 521 Sato, Tamaki. 2005. “A New Polycotyloid Plesiosaur (Reptilia: Sauropterygia) from the Upper Cretaceous  
522 Bearpaw Formation in Saskatchewan, Canada.” *Journal of Paleontology* 79 (5): 969–80.  
523 <https://www.jstor.org/stable/4095068>.
- 524 Sato, Tamaki, Takuya Konishi, R. Hirayama, and Michael W. Caldwell. 2012. “A Review of the Upper  
525 Cretaceous Marine Reptiles from Japan.” *Cretaceous Research* 37: 319–40.  
526 <https://doi.org/10.1016/j.cretres.2012.03.009>.
- 527 Sax, Dov F., and Steven D. Gaines. 2003. “Species Diversity: From Global Decreases to Local Increases.”  
528 *Trends in Ecology & Evolution* 18 (11): 561–66. [https://doi.org/10.1016/S0169-5347\(03\)00224-6](https://doi.org/10.1016/S0169-5347(03)00224-6).
- 529 Scheyer, Torsten M., Carlo Romano, Jim Jenks, and Hugo Bucher. 2014. “Early Triassic Marine Biotic  
530 Recovery: The Predators’ Perspective.” *PLOS ONE* 9 (3): e88987.  
531 <https://doi.org/10.1371/JOURNAL.PONE.0088987>.

- 532 Schneider, Caroline A, Wayne S Rasband, and Kevin W Eliceiri. 2012. “NIH Image to ImageJ: 25 Years of  
533 Image Analysis.” *Nature Methods* 9 (7): 671–75. <http://www.ncbi.nlm.nih.gov/pubmed/22930834>.
- 534 Schumacher, Bruce A. 2011. “A ‘Woollgari -Zone Mosasaur’ (Squamata; Mosasauridae) from the Carlile  
535 Shale (Lower Middle Turonian) of Central Kansas and the Stratigraphic Overlap of Early Mosasaurs and  
536 Pliosaurid Plesiosaurs.” *Transactions of the Kansas Academy of Science* 114 (1 & 2): 1–14.  
537 <https://doi.org/10.1660/062.114.0101>.
- 538 Scotese, Christopher R. 2014. “Atlas of Late Cretaceous Paleogeographic Maps.” *Atlas of Late Cretaceous*  
539 *Paleogeographic Maps 2* (The Cretaceous): Maps 16-22.
- 540 Simões, Tiago R., Oksana Vernygora, Ilaria Paparella, Paulina Jimenez-Huidobro, and Michael W. Caldwell.  
541 2017. “Mosasauroid Phylogeny under Multiple Phylogenetic Methods Provides New Insights on the  
542 Evolution of Aquatic Adaptations in the Group.” *PLoS ONE* 12 (5): 1–20.  
543 <https://doi.org/10.1371/journal.pone.0176773>.
- 544 Slattery, Joshua, William A. Cobban, Kevin C. McKinnery, Peter Jürgen Harries, and Ashley L. Sandness.  
545 2013. “Early Cretaceous to Paleocene Paleogeography of the Western Interior Seaway: The Interaction  
546 of Eustasy and Tectonism.” *Wyoming Geological Association Guidebook*, 22–60.  
547 <https://doi.org/10.13140/RG.2.1.4439.8801>.
- 548 Strong, Catherine R.C., Michael W. Caldwell, Takuya Konishi, and Alessandro Palci. 2020. “A New Species  
549 of Longirostrine Plioplatecarpine Mosasaur (Squamata: Mosasauridae) from the Late Cretaceous of  
550 Morocco, with a Re-Evaluation of the Problematic Taxon ‘Platecarpus’ Ptychodon.” *Journal of*  
551 *Systematic Palaeontology* 0 (0): 1–36. <https://doi.org/10.1080/14772019.2020.1818322>.
- 552 Stubbs, Thomas L., and Michael J. Benton. 2016. “Ecomorphological Diversifications of Mesozoic Marine  
553 Reptiles: The Roles of Ecological Opportunity and Extinction.” *Paleobiology* 42 (4): 547–73.  
554 <https://doi.org/10.1017/PAB.2016.15>.
- 555 Stubbs, Thomas L., Stephanie E. Pierce, Armin Elsler, Philip S.L. Anderson, Emily J. Rayfield, and Michael  
556 J. Benton. 2021. “Ecological Opportunity and the Rise and Fall of Crocodylomorph Evolutionary

- 557 Innovation.” *Proceedings of the Royal Society B* 288 (1947). <https://doi.org/10.1098/RSPB.2021.0069>.
- 558 Stubbs, Thomas L., Stephanie E. Pierce, Emily J. Rayfield, and Philip S.L. Anderson. 2013. “Morphological  
559 and Biomechanical Disparity of Crocodile-Line Archosaurs Following the End-Triassic Extinction.”  
560 *Proceedings of the Royal Society B: Biological Sciences* 280 (1770).  
561 <https://doi.org/10.1098/RSPB.2013.1940>.
- 562 Tanimoto, M. 2005. “Mosasaur Remains from the Upper Cretaceous Izumi Group of Southwest Japan.”  
563 *Netherlands Journal of Geosciences / Geologie En Mijnbouw* 84 (3): 373–78.  
564 <https://doi.org/10.1017/S0016774600021156>.
- 565 Tutin, Samuel L., and Richard J. Butler. 2017. “The Completeness of the Fossil Record of Plesiosaurs, Marine  
566 Reptiles from the Mesozoic.” *Acta Palaeontologica Polonica* 62 (3): 563.  
567 <https://doi.org/10.4202/APP.00355.2017>.
- 568 Upchurch, P., P. D. Mannion, R. B. J. Benson, R. J. Butler, and M. T. Carrano. 2011. “Geological and  
569 Anthropogenic Controls on the Sampling of the Terrestrial Fossil Record: A Case Study from the  
570 Dinosauria.” *Geological Society, London, Special Publications* 358 (1): 209–40.  
571 <https://doi.org/10.1144/SP358.14>.
- 572 Vavrek, M. J., and H. C. Larsson. 2010. “Low Beta Diversity of Maastrichtian Dinosaurs of North America.”  
573 *Proceedings of the National Academy of Sciences of the United States of America* 107 (18): 8265–68.  
574 <https://doi.org/10.1073/PNAS.0913645107>.
- 575 Wilberg, Eric W. 2017. “Investigating Patterns of Crocodyliform Cranial Disparity through the Mesozoic and  
576 Cenozoic.” *Zoological Journal of the Linnean Society* 181 (1): 189–208.  
577 <https://doi.org/10.1093/ZOOLINNEAN/ZLW027>.
- 578 Zaffos, Andrew, Seth Finnegan, and Shanan E. Peters. 2017. “Plate Tectonic Regulation of Global Marine  
579 Animal Diversity.” *Proceedings of the National Academy of Sciences* 114 (22): 5653–58.  
580 <https://doi.org/10.1073/PNAS.1702297114>.

582 **Tables**

583 **Table 1.** Functional traits derived from linear measurements of mosasaurid skulls and jaws. Definitions,  
 584 calculations and diagrammatic representations for each trait can be found in the Supplementary Information 3:  
 585 Functional Ratios. % cov. = percentage of specimens represented by each trait. Percentages in italics fall  
 586 outside the completeness threshold of 40%.

Character	Function	% cov.
jaw depressor lever arm ratio	proxy for jaw opening mechanical advantage	77.2
jaw adductor lever arm ratio	proxy for jaw closing mechanical advantage	73.7
functional tooththrow	defines proportion of jaw used for prey capture/processing	89.5
jaw robusticity	proxy for jaw bending resistance	85.9
supratemporal fenestra area	cross-sectional area of jaw adductor muscles	77.2
longirostry	defines hydrodynamic potential of pre-orbital snout	87.7
gullet size	proxy for volume of water expulsion, prey size etc.	80.7
tooth crown shape	proxy for tooth narrowing; hard vs. soft food items	96.5
tooth blade shape	describes dental compression; conical vs. blade-like teeth	61.4
tooth crown curvature	describes dental recurvature	96.5
nares position	proxy for ease of inhalation during steady-state swimming	78.9
relative orbit size	defines importance of vision for taxon	75.4
pupil size (sclerotic ring diameter)	defines amount of light able to enter the pupil	15.8
tympanic resonator area	proxy for area of quadrate available as resonator	73.7
premaxillary elongation	proxy for area available for anterior pressure sensation	75.4
parietal foremen	proxy for relative size of pineal eye	70.2

587

588

589 **Table 2.** Mosasaurid population disparity (alpha, gamma and beta) from Early Campanian to Late  
 590 Maastrichtian. Sum of variances metric used. Highest mean disparity values highlighted in bold. WIS =  
 591 Western Interior Seaway; NTP = Northern Tethys Province; STP = Southern Tethys Province; WP =  
 592 Weddellian Province.

Disparity		Early Campanian	Late Campanian	Early Maastrichtian	Late Maastrichtian
gamma ( $\gamma$ )		18.90	19.30	<b>21.19</b>	20.12
alpha ( $\alpha$ )	Mean	15.94	16.17	<b>19.26</b>	14.63
	WIS	18.43	<b>19.57</b>	18.52	9.76
	NTP	22.03	21.60	<b>23.35</b>	17.50
	STP	10.22	10.44	<b>22.04</b>	21.51
	WP	13.07	13.06	<b>13.13</b>	9.75
beta ( $\beta$ )		1.186	1.194	1.100	<b>1.375</b>

593

594

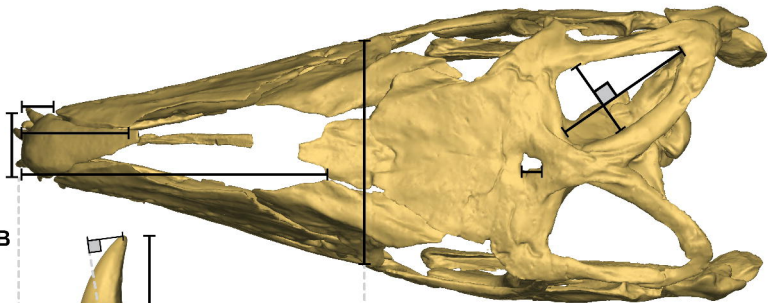
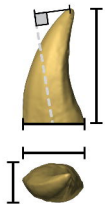
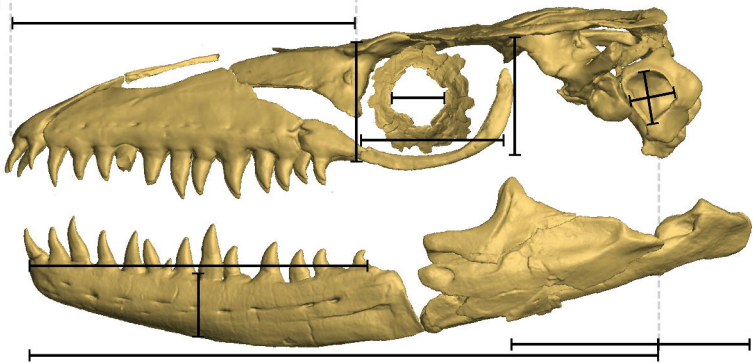


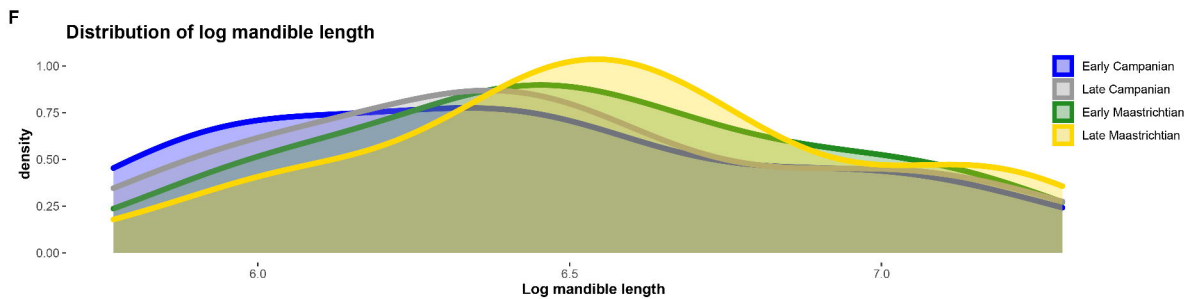
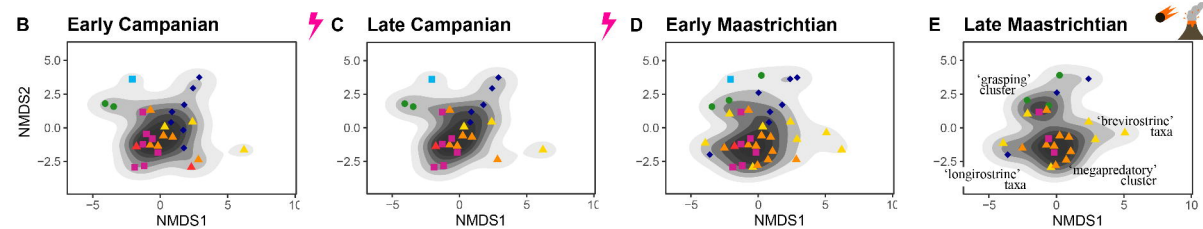
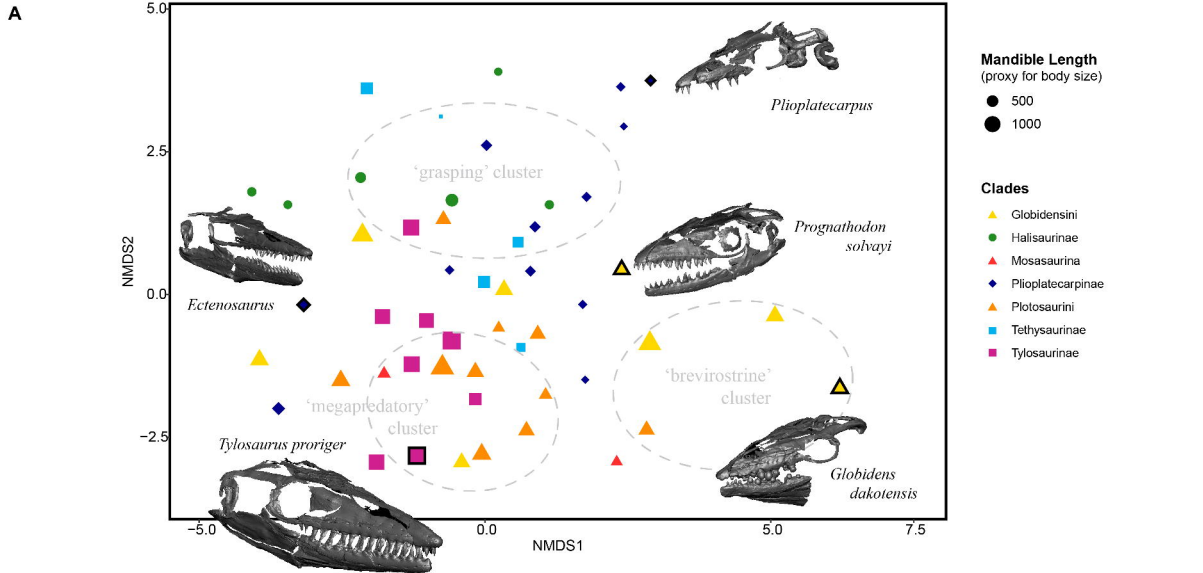
595 **Figure Legends**

596 **Figure 1.** Linear measurements of the mosasaurid skull used for quantitative trait comparisons and disparity  
597 analyses. Measurements on the skull and exemplar dentition are shown: **(A)** skull in dorsal aspect, **(B)**  
598 dentition in lateral and occlusal aspect, **(C)** skull in left lateral aspect. Filled squares denote measurements  
599 taken perpendicular to one another or to the edge of a bone. Black lines describe measurements used for trait  
600 quantification; dotted grey lines are used to clarify where specific measurements are recorded from and to.  
601 Functional traits and their ecomorphological importance are presented in Table 1. Models based on IRSNB  
602 R33b *Prognathodon solvayi*.

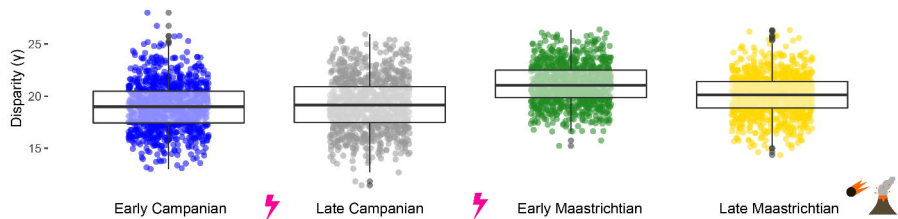
603 **Figure 2.** Functional ecomorphospace and size distribution in mosasaurids. Functional ecomorphospace  
604 occupation (based on NMDS axes) by all mosasaurids in the sample **(A)** with ecomorphological clusters and  
605 representative 3D models of skulls. Data points outlined in bold represent the placement of exemplar skulls;  
606 data point size represents relative skull size (based on mandible length). Functional ecomorphospace for each  
607 time bin through the Campanian-Maastrichtian **(B-E)** demonstrating changes in density and isolation of  
608 ecomorphological clusters in Late Maastrichtian **(E)**. Size distribution of mosasaurids through the Campanian-  
609 Maastrichtian **(F)** demonstrating shifts in the density of small and mid-sized mosasaurids from Early  
610 Campanian (ECam) to Late Maastrichtian (LMaa).

611 **Figure 3.** Global and provincial mosasaurid craniodental disparity through time. Global ( $\gamma$ ) craniodental  
612 disparity of mosasaurids from Early Campanian to Late Maastrichtian **(A)** presented alongside raw sample  
613 diversity and provincial ( $\alpha$ ) disparity for the Maastrichtian of the Western Interior Seaway **(B)**, Northern **(C)**  
614 and Southern **(D)** Tethys Provinces, and Weddellian Province **(E)**. Approximate extent of provincial regions  
615 projected onto palaeomap, estimated for mid-Maastrichtian (72 Ma). Disparity estimates were generated using  
616 the sum of variances (SoV) metric; significant differences were recovered between all sequential time bins for  
617 both global and provincial datasets using pairwise Wilcoxon testing (see also Supplementary Table S1 & S3).  
618 Palaeomap provided by CR Scotese (PALEOMAP atlas for ArcGIS) (Scotese 2014).

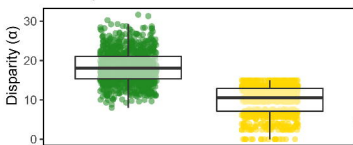
**A****B****C**



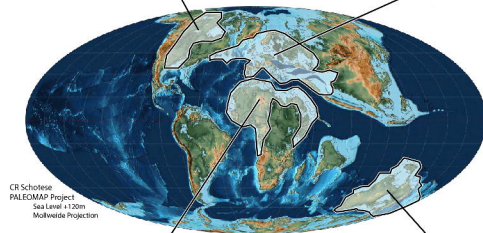
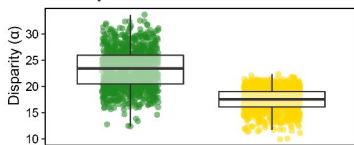
## A Global Mosasaurid Disparity



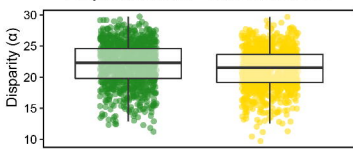
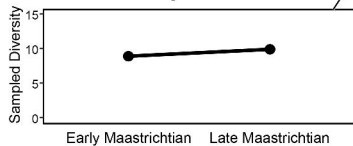
## B Western Interior Seaway



## C Northern Tethys Province



## D Southern Tethys Province



## E Weddellian Province

